100, 200, and 300 K for $Sr_3Co_2Fe_{24}O_{41}$ polycrystalline samples sintered in oxygen. As seen in Fig. 2a, the magnetization increases in two steps up to the saturation magnetization. As the magnetic field increases, the magnetization shows a rapid increase from 0 to ~0.1 T, gently increases from ~0.1 T to ~0.7 T, and then is almost saturated at around 1 T. These features can be explained by the transformation from the transverse conical ordered state (Fig. 1b) into the ferromagnetic state (Fig. 1c). These anomalies in the magnetization accompany magnetoelectric effects. As displayed in Fig. 2b, there is almost no spontaneous polarization at zero magnetic fields. By applying a magnetic field, the electric polarization appears and shows a rapid increase up to ~0.2 T. With the further increase of the magnetic field, the electric polarization reaches a maximum at 0.25~0.3 T (23 μC/m2 at 100 K) and then starts to decrease. Finally, the electric polarization vanishes at around 1 T where the system becomes a simple ferrimagnet. These results demonstrate that the Z-type $Sr_3Co_2Fe_{24}O_{41}$ exhibits the magnetoelectric effect at a wide range of temperatures including room temperature. The room-temperature ME effect can be understood in terms of the appearance of the electric polarization which is induced by the transverse conical magnetic structure through the spin-current mechanism [8].

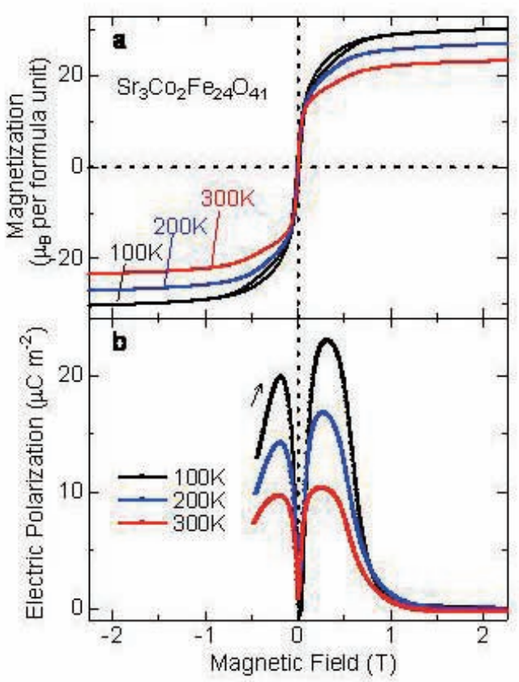

Fig.2 Magnetic-field dependence of **(a)** magnetization and **(b)** electric polarization at 100, 200, and 300 K for a polycrystalline sample of $Sr_3Co_2Fe_{24}O_{41}$ sintered in oxygen.

In the Z-type hexaferrite, a potential use of the magnetoelectric effect in practical device applications is demonstrated, i.e., a sequential switching of the electric polarization by oscillating magnetic fields between 0 and 0.25 T (Fig. 3a) at 300 K. As displayed in Fig. 3b, reproducible variations of the electric polarization were observed without any decays in their magnitudes. In addition, the signs of the magnetoelectric signals are switchable with the polarity of a poling electric field (Compare Figs. 3b and 3d). Thus, the low-field magnetoelectric effect observed in the Z-type hexaferrite ceramics at room temperature has the promise of practical device applications including non-volatile memory where information is stored as electrically-detectable and -controllable spin-helicity, as schematically illustrated in Fig. 3e.

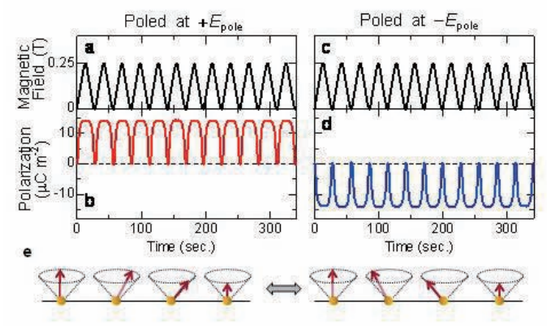

Fig.3 Room-temperature magnetoelectric effect of $Sr_3Co_2Fe_{24}O_{41}$ polycrystalline ceramics sintered in oxygen. Oscillating electric polarization responding to periodically varying magnetic fields between 0 and 0.25 T **(a,c)**. The data for **(b)** and **(d)** were obtained after poling at plus and minus electric fields, respectively. **(e)** Schematic illustrations of electrically-detectable and -controllable spin-helicity.

Summary

A Z-type hexaferrite $Sr_3Co_2Fe_{24}O_{41}$ has been found to exhibit a low-field magnetoelectric effect "at room temperature". The discovery clearly demonstrates the magnetic-field control of ferroelectricity at "room temperature", and represents an important step toward practical applications using the magnetoelectric effect. The results presented here provide the promise of practical magnetoelectric device applications including non-volatile memory where information is stored as electrically-detectable and -controllable spin-helicity.

References

[1] W. Erenstein, N. D. Mathur, and J. F. Scott , *Nature* 442,759 (2006).
[2] S. W. Cheong and M. V. Mostovoy, *Nature Mater*. 6, 13 (2007).
[3] T. Kimura, T. Goto, H. Shintani, K. Ishizaka, T. Arima, and Y. Tokura, *Nature* 426:55 (2003).
[4] J. Smit and H. P. J. Wijn, *Ferrites*. Eindhoven, The Netherlands: Phillips Tech. Libr. (1959).
[5] T. Kimura, G. Lawes, and A. P. Ramirez, *Phys. Rev. Lett*. 94, 137201 (2005).
[6] Y. Kitagawa, Y. Hiraoka, T. Honda, T. Ishikura, H. Nakamura, and T. Kimura, *Nature Mater*. 9, 797 (2010).
[7] M. Soda, T. Ishikura, H. Nakamura, Y. Wakabayashi, and T. Kimura, *Phys. Rev*. Lett. 106, 087201 (2011).
[8] H. Katsura, N. Nagaosa, and A. V. Balatsky, *Phys. Rev. Lett*. 95, 057205 (2005).

In the Z-type hexaferrite, a potential use of the magnetoelectric effect in practical device applications is demonstrated,

Surface-Plasmon Holography with White-Light Illumination

Paper in journals: this is the first page of a paper published in ***Science***.
[*Science*] 332, 218(2011)

REPORTS

We have constrained the parameters of the BC pair by modeling the short-period eclipses in the Kepler band using the Ajketbop code (*15*, *17*). The ratio of the radii of the B and C components is poorly constrained at present, partly because of the low sampling rate of the Kepler LC data. The A component contributes 99.29% of the system light in the Kepler passband, and the BC pair contribute 0.44% and 0.27%, respectively. Taking the *V*-band absolute magnitude of HD 181068 A to be $M_V(A) = -0.3$ and assuming that our results for the Kepler passband are representative of the *V* band, we find $M_V(B) = 5.6$ and $M_V(C) = 6.1$. Such absolute magnitudes indicate spectral types of G8 V and K1 V for stars B and C, respectively (*18*). Because we do not have independent measurements of T_{eff} for the BC pair, we can only estimate their masses based on their spectral types. This indicates that their masses are about 0.7 ± 0.1 $M_\odot$ each (*6*).

One puzzling feature of the system is the short-period fluctuations that have the largest amplitudes when the BC pair is behind star A, while remaining apparent with a slowly changing amplitude in all the other phases of the wide orbit. We have investigated this variability of HD 181068 A with a detailed frequency analysis and a comparison to other red giant stars that have similar properties (*6*). The frequency content of the light curve suggests an intimate link to tidal effects in the triple system, with the first four dominant peaks in the power spectrum identifiable as simple linear combinations of the two orbital frequencies. On the other hand, solarlike oscillations (meaning those excited by near-surface convection, as in the Sun but also observed in red giants) that are expected to produce an equidistant series of peaks in the power spectrum are not visible, even though all stars with similar parameters in the Kepler database do show clear evidence of these oscillations. In other words, the convectively driven solarlike oscillations that we would expect to see in a giant of this type seem to have been suppressed (*5*).

In a recent compilation of 724 triple stars (*19*), there is only one system with an outer orbital period shorter than that of HD 181068 (λ Tau, for which P_{out} = 33.03 days). Carter *et al.* (*20*) reported the discovery of KOI-126 with a similarly short outer period (P_{out} = 33.92 days). Extremely compact hierarchical triple systems form a very small minority of hierarchical triplets, with only 7 of the catalogized 724 systems having outer periods shorter than 150 days. Furthermore, HD 181068 and KOI-126 have the highest outer mass ratios [~ 2.1 and 3, defined as $m_A/(m_B + m_C)$] among the known systems. In 97% of the known hierarchical triplets before the Kepler era, the mass of the close binary exceeded that of the wider companion, and even the largest outer mass ratio remained under 1.5. It is not yet clear whether this rarity of such systems is caused by an observational selection effect or has an underlying stellar evolutionary or dynamical explanation.

Its properties make HD 181068 an ideal target for dynamical evolutionary studies and for testing tidal friction theories. Because of its compactness and its massive primary, we can expect short-term orbital element variations on two different time scales of 46 days (i.e., with period of $P_{A\text{-}BC}$) and about 6 years ($P_{A\text{-}BC}^2/P_{BC}$), the time scale of the classical apsidal motion and nodal regression (*21*), which for the triply eclipsing nature could be observed relatively easily.

References and Notes

1. W. J. Borucki *et al.*, *Science* **327**, 977 (2010).
2. D. G. Koch *et al.*, *Astrophys. J.* **713**, L79 (2010).
3. J. M. Jenkins *et al.*, *Astrophys. J.* **713**, L87 (2010).
4. J. M. Jenkins *et al.*, *Astrophys. J.* **713**, L120 (2010).
5. P. Guillout *et al.*, *Astron. Astrophys.* **504**, 829 (2009).
6. Materials and methods are available as supporting material on *Science* Online.
7. Available at http://archive.stsci.edu/kepler/.
8. M. J. Ireland *et al.*, in *Optical and Infrared Interferometry*, M. Schöller, W. C. Danchi, F. Delplancke, Eds., vol. 7013 of *Proceedings of the SPIE* (Society of Photo-Optical Instrumentation Engineers, Bellingham, WA, 2008), pp. 701324–701324-10.
9. T. A. ten Brummelaar *et al.*, *Astrophys. J.* **628**, 453 (2005).
10. R. Hanbury Brown *et al.*, *Mon. Not. R. Astron. Soc.* **167**, 475 (1974).
11. F. van Leeuwen, *Hipparcos, the New Reduction of the Raw Data* (Astrophysics and Space Science Library, Springer, Berlin, 2007), vol. 350.
12. O. C. Wilson, M. K. V. Bappu, *Astrophys. J.* **125**, 661 (1957).
13. G. Pace, L. Pasquini, S. Ortolani, *Astron. Astrophys.* **401**, 997 (2003).
14. A. Pietrinferni, S. Cassisi, M. Salaris, F. Castelli, *Astrophys. J.* **612**, 168 (2004).
15. L. Girardi, *Mon. Not. R. Astron. Soc.* **308**, 818 (1999).
16. J. Southworth, J. Zucker, P. F. L. Maxted, B. Smalley, *Mon. Not. R. Astron. Soc.* **355**, 986 (2004).
17. J. Southworth, B. Smalley, P. F. L. Maxted, A. Claret, P. B. Etzel, *Mon. Not. R. Astron. Soc.* **363**, 529 (2005).
18. A. N. Cox, *Allen's Astrophysical Quantities* (Springer, New York, 2000).
19. A. A. Tokovinin, *Mon. Not. R. Astron. Soc.* **389**, 925 (2008).
20. J. A. Carter *et al.*, *Science* **331**, 562 (2011); 10.1126/science.1201274.
21. E. W. Brown, *Mon. Not. R. Astron. Soc.* **97**, 62 (1936).

A.D. is a Magyary Zoltán Postdoctoral Research Fellow. Funding for this Discovery mission is provided by NASA's Science Mission Directorate. The authors gratefully acknowledge the entire Kepler team, whose outstanding efforts have made these results possible. This project has been supported by Hungarian Scientific Research Fund (OTKA) grants K76816, K83790, and MB08C 81013; the "Lendület" Program of the Hungarian Academy of Sciences; and the Magyary Zoltán Higher Educational Public Foundation. The DAO observations were supported by an American Astronomical Society Small Research Grant. The CHARA Array is owned by Georgia State University. Additional funding for the CHARA Array is provided by NSF under grant AST09-08253, the W. M. Keck Foundation, and the NASA Exoplanet Science Center. TLS observations were done as a part of the Deutsche Forschungsgemeinschaft grant HA 3279/5-1. For her research, C.A. received funding from the European Research Council (ERC) under the European Community's Seventh Framework Programme (FP7/2007-2013)/ERC grant agreement no. 227224 (Prosperity).

Supporting Online Material

www.sciencemag.org/cgi/content/full/332/6026/216/DC1
Materials and Methods
Figs. S1 to S3
Tables S1 to S3
References
SOM Data

15 December 2010; accepted 3 March 2011
10.1126/science.1201762

Surface-Plasmon Holography with White-Light Illumination

Miyu Ozaki,[1,2] Jun-ichi Kato,[1] Satoshi Kawata[1,3]*

The recently emerging three-dimensional (3D) displays in the electronic shops imitate depth illusion by overlapping two parallax 2D images through either polarized glasses that viewers are required to wear or lenticular lenses fixed directly on the display. Holography, on the other hand, provides real 3D imaging, although usually limiting colors to monochrome. The so-called rainbow holograms—mounted, for example, on credit cards—are also produced from parallax images that change color with viewing angle. We report on a holographic technique based on surface plasmons that can reconstruct true 3D color images, where the colors are reconstructed by satisfying resonance conditions of surface plasmon polaritons for individual wavelengths. Such real 3D color images can be viewed from any angle, just like the original object.

Noble metal films, such as silver and gold foil, contain free electrons that collectively oscillate and propagate as the surface wave in optical frequency region. The quantum of this surface wave is called surface plasmon polariton (SPP) (*1*). The electromagnetic field generated by SPP can be enhanced and strongly confined spatially in the near field (with the distance less than the wavelength) from the metal surface as a nonirradiative evanescent field (*2*, *3*). The ability to confine and enhance the optical field to the vicinity of the metal surface or nanometal particle has been applied to immuno-sensor (*4*), fluorescence sensor (*5*), solar cell (*6*), plasmonic laser (*7*, *8*), nanomicroscopy (*9*, *10*), super-lens (*11*, *12*) and photodynamic cancer cell treatment (*13*).

We report an application of SPP to three-dimensional (3D) color holography with white-

[1]RIKEN, Wako, Saitama 351-0198, Japan. [2]Department of Robotics and Mechatronics, Tokyo Denki University, Chyoda-ku, Tokyo 101-8457, Japan. [3]Department of Applied Physics and Photonics Advanced Research Center, Osaka University, Suita, Osaka, 565-0871, Japan.
*To whom correspondence should be addressed. E-mail: kawata@skawata.com

▲From ***Science***, 332, Miyu Ozaki et al., Surface-Plasmon Holography with White-Light Illumination, 218(2011). Reprinted with permission from AAAS.

The following is a comment on the published paper shown on the preceding page.

Surface-Plasmon Holography

KAWATA Satoshi
(Graduate School of Engineering)

Making holograms look more real

A full-color three-dimensional hologram has been created by harnessing electron density waves in thin metal films. Although human vision is capable of perceiving objects in three dimensions (3D), we spend much of our day looking at two-dimensional screens. The latest televisions and monitors can trick us into perceiving depth, by presenting different images to our left and right eyes, but they require special-purpose glasses, or specialized large-area lenses applied directly to the screen.

Holographic 3D imaging, on the other hand, presents a 'true' representation of an object by exactly reconstructing the light rays that would come from that object if it were present. However, integrating color into 3D holograms has proved a challenge. Consequently, holograms are usually either monochromatic, or—as in the case of credit card holograms—colored in a way that does not correspond to the real object. Now, creating true, 3D color holograms has become possible using a technique developed by Satoshi Kawata and colleagues at the RIKEN Advanced Science Institute in Wako.

The researchers' hologram consists of a periodic grating, which is encoded with an interference pattern and covered with a thin film of silver. As with other holograms, when properly illuminated at a later time, the hologram can recreate the light rays that would result from the original object if it were present. The innovation comes in how this grating interacts with the silver film, whose electrons can be excited into density waves called surface plasmon polaritons (SPPs). SPPs are associated with a short-range, non-radiative electromagnetic field. When this field interacts with the grating, it is converted into visible light that can be observed by a viewer at a distance.

Critically, the nature of the SPPs excited in the silver depends on the angle of light that excites them. Therefore a particular type of SPP can be created by illuminating the film at a particular angle, and this in turn leads to a particular image being observed by the viewer. By encoding red, green and blue images into their grating, and then illuminating the grating and silver film simultaneously with three light beams at different angles, Kawata and colleagues produced a full-color hologram (Fig. 2A).

To make the hologram easier to operate, the researchers also coated their silver film with a layer of silicon dioxide. This increased the separation between the angles of the incoming beams, and reduced the angular precision required. The team notes that the hologram works with beams of white light, and does not suffer from the 'ghosting' that is apparent with credit card holograms.

(From RIKEN RESEARCH HIGHLIGHT,Courtesy of RIKEN)

Plasmon Holography in Color

Noble metal films, such as silver and gold foil, contain free electrons that collectively oscillate and propagate as the surface wave in optical frequency region. The quantum of this surface wave is called surface plasmon polariton (SPP) (1). The electromagnetic field generated by SPP can be enhanced and strongly confined spatially in the near field (with the distance less than the wavelength) from the metal surface as a nonirradiative evanescent field (2, 3). The ability to confine and enhance the optical field to the vicinity of the metal surface or nanometal particle has been applied to immuno-sensor (4), fluorescence sensor (5), solar cell (6), plasmonic laser (7, 8), nanomicroscopy (9, 10), super-lens (11, 12) and photodynamic cancer cell treatment (13).

We report an application of SPP to threedimensional (3D) color holography with white-light illumination. The first idea to use plasmons for holography was published as a reflection type by Cowan (14), and since then authors have reported holographic reconstruction of transmission type (15–17). In those configurations, plasmons have been used for enhancing the diffraction efficiency. In this report, we use color selectivity of SPPs for holographic color reconstruction with white-light illumination.

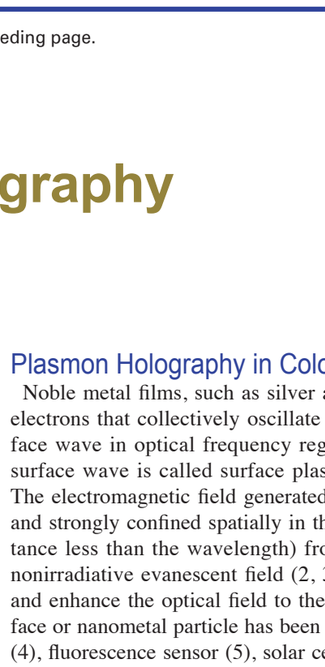

Fig.1
Surface plasmon hologram and its color reconstruction with white-light illumination. (A) The SPP hologram is illuminated by white light at a given angle θ in high-index medium. Surface plasmons of a selected color are excited and diffracted by the SPP hologram to reconstruct the wavefront of the object. (B) Dispersion curve of SPP hologram in reconstruction as a function of incident angle of white light. The 3D images of red, green and blue cranes made of papers, are obtained at different angles with white light illumination. This curve was obtained through the calculation based on Fresnel's equations. (C) Reconstruction of a color object through SPP hologram. The hologram is illuminated simultaneously with a white light in three directions at different angles θ and φ for each.

We recorded the hologram on a photoresist as an interference pattern between a light field coming from the object as scattered light and the unscattered reference beam. Exposure was repeated three times with rotation of the illumination angle for a single color hologram recording. Instead of rotation, one can also use three lasers simultaneously to obtain the hologram in a single exposure. A thin metal film is then coated on the photoresist hologram,which is precoated on a glass plate. For image reconstruction, the SPP is excited by a color component of white light that is incident on the metal film through a prism with an angle satisfying the condition of total internal reflection (Fig. 1A). The SPP associates with a nonradiative evanescent light wave on metal film and then is converted by the grating component of hologram into a radiative light field, which represents the reconstructed wavefront of light that scattered at the object. The reconstruction of the prerecorded object is seen with the eyes through an SPP hologram in color. The reference beam or the zeroth-order diffraction as background beam does not exist in reconstruction for this configuration because the illumination of the hologram is made by total internal reflection.

Figure 1B shows the dispersion curve of SPP with wavelength λ as a function of the incident angle θ of illumination (excitation). This relationship is given as

$$\theta = \sin^{-1}\left(\frac{1}{n_{glass}}\sqrt{\frac{n_m^2 n(\lambda)^2}{n_m^2 + n(\lambda)^2}}\right) \quad (1)$$

where n_{glass}, n_m, and $n(\lambda)$ are the refractive index of the glass substrate, effective index of the medium on the metal surface, and the index of metal (which is a function of λ), respectively (2).

Individual colors are reconstructed by illumination at corresponding incident angles by satisfying the above relationship for each color. Figure 1C shows the optical setup for reconstructing a three-color object in different azimuthal and incident angle sets [(φ_R, θ_R), (φ_G, θ_G), and (φ_B, θ_B)] with white-light illumination.

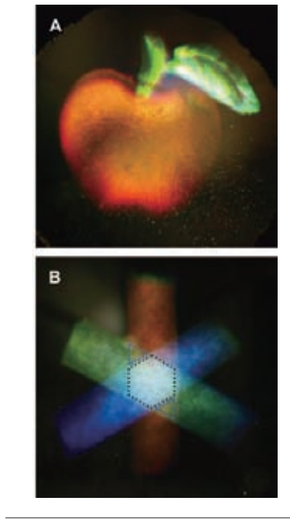

Fig.2 Reconstruction of three-dimensional color objects through surface plasmon holograms. (A) Red apple with green leaf in three dimensions. (B) Color bar recorded three times with red, green, and blue by rotating the bar by 120° for each color. In the center where three colors overlap, a hexagonal area is reconstructed as white, while yellow triangles are reconstructed where red and green overlap.

Reconstruction of an object, an apple with a leaf, is seen in 3D from the thin film plasmon hologram (Fig. 2A) (18). A movie of the object taken with a camera moving around the object is provided in the supporting online material. For plasmon color holography, the adjustment of the white color balance is important for representing the natural color of an object or a scene. We obtained the white color balance by carefully controlling the power of the laser with multiple exposures for red (R), green (G), and blue (B). Figure 2B shows an image of a bar taken by three-time exposure in R, G, and B; each exposure was made by rotating the object (bar) and by taking shots at every 120° of rotation. It includes a white hexagon in the center where all three colors overlap and yellow triangles where red and green bars overlap. For reconstruction of the object, a 100-W Halogen lamp is used.

Discussions

The results show that plasmon color holography provides a view of an object or a scene seen naturally and vitally with white-light illumination. A typical amplitude modulation in plasmon hologram is ~25 nm, which is much thinner comparedwith Lippmann-Denisyuk's color hologram (19) based on Bragg diffraction in volume. The rainbow holograms mounted, for example, on credit cards (20) also reconstruct with white light, where color varies with viewing angle but not with the color distribution in the object. Plasmon holography is advantageous in terms of background-beam–free reconstruction because the illumination light is totally reflected back at the hologram (21). Plasmon holography does not suffer from the ghost produced by the diffraction of ambient light or higher orders of diffraction, because those components are not coupled with SPPs.

References

[1] J. Heber, Nature 461, 720 (2009).
[2] H. Raether, Surface Plasmons on Smooth and Rough surfaces and on Gratings (Springer, Berlin, 1988).
[3] S. Kawata, Near Field Optics and Surface Plasmon Polaritons (Springer, Berlin, 2001).
[4] B. Liedberg, C. Nylander, I. Lunström, Sens. Actuators 4, 299 (1983).
[5] H. Kano, S. Kawata, Opt. Lett. 21, 1848 (1996).
[6] V. E. Ferry, L. A. Sweatlock, D. Pacifici, H. A. Atwater, Nano Lett. 8, 4391 (2008).
[7] T. Okamoto, F. H'Dhili, S. Kawata, Appl. Phys. Lett. 85, 3968 (2004).
[8] N. I. Zheludev, S. L. Prosvirnin, N. Papasimakis, V. A. Fedotov, Nat. Photonics 2, 351 (2008).
[9] S. Kawata, Y. Inouye, P. Verma, Nat. Photonics 3, 388 (2009).
[10] N. Hayazawa, Y. Inouye, Z. Sekkat, S. Kawata, Opt. Commun. 183, 333 (2000).
[11] J. B. Pendry, Phys. Rev. Lett. 85, 3966 (2000).
[12] N. Fang, H. Lee, C. Sun, X. Zhang, Science 308, 534 (2005).
[13] C. Loo, A. Lowery, N. Halas, J. West, R. Drezek, Nano Lett.5, 709 (2005).
[14] J. J. Cowan, Opt. Commun. 5, 69 (1972).
[15] S. Maruo, O. Nakamura, S. Kawata, Appl. Opt. 36, 2343(1997).
[16] G. P. Wang, T. Sugiura, S. Kawata, Appl. Opt. 40, 3649(2001).
[17] M. Ozaki, J. Kato, R. Furutani, S. Kawata, J. Jpn. Soc.Precision Eng. 74, 1113 (2008).
[18] Materials and methods are available as supportingmaterials on Science Online.
[19] Yu. N. Denisyuk, Sov. Phys. Dokl. 7, 543 (1962).
[20] S. A. Benton, J. Opt. Soc. Am. 59, 1545 (1969).
[21] O. Bryngdahl, J. Opt. Soc. Am. 59, 1645 (1969).